

# DEFENCE S&T TECHNICAL BULLETIN

VOL. 12 NUM. 1 YEAR 2019 ISSN 1985-6571

## CONTENTS

Discriminating Closely Spaced Aircrafts Using Time Difference of Arrival (TDOA) Based Association Algorithm <i>Abdulmalik Shehu Yaro, Ahmad Zuri Sha'ameri &amp; Sa'id Musa Yarima</i>	1 - 15
A Review of Copter Drone Detection Using Radar Systems <i>Surajo Alhaji Musa, Raja Syamsul Azmir Raja Abdullah, Aduwati Sali, Alyani Ismail, Nur Emileen Abdul Rashid, Idnin Pasya Ibrahim &amp; Asem Ahmad Salah</i>	16 - 38
Spaceborne Synthetic Aperture Radar (SAR) Sensors in Low Earth Orbit (LEO) for Real-Time Detection and Monitoring of Floods <i>Arun Kumar Verma, Ranbir Nandan &amp; Aditi Verma</i>	39 - 50
Development of HF Modelling in Peninsular Malaysia During the Rise of Solar Cycle 24 <i>Rafidah Abd Malik, Mardina Abdullah, Sabirin Abdullah, Yokoyama Tatsuhiro &amp; Clara Y. Yatini</i>	51 - 60
Review of Machine Learning Based Hardware Trojan Detection Methods <i>Chee Hoo Kok, Chia Yee Ooi, Michiko Inoue, Nordinah Ismail, Mehrdad Moghbel &amp; Hau Sim Choo</i>	61 - 78
A Message Cryptography Technique Using DNA Based Hybrid Approach <i>Vaibhav Godbole</i>	79 - 90
Investigation of Vehicle Occupant Response Subjected to Under-Vehicle Explosion <i>Khalis Suhaimi, Risby Mohd Sohaimi, Muhammad Fahmi Md. Isa, Muhd Azhar Abu Bakar, Norazman Mohamad Nor, Ariffin Ismail &amp; Victor Feisal Knight</i>	91 - 100
Optimisation of Hybrid Composite Reinforced Carbon and Glass Using AHP Method <i>Nur Aizatul 'Ain Md Zahir, Ahmad Fuad Ab Ghani, Mohd Ahadlin Mohd Daud, Sivakumar Dhar Malingam &amp; Ridzuan Mansur</i>	101 - 102
The Influence of Fibre Stacking Configurations on the Indentation Behaviour of Pineapple Leaf / Glass Fibre Reinforced Hybrid Composites <i>Ng Lin Feng, Sivakumar Dhar Malingam, Kathiravan Subramaniam, Mohd Zulkefli Selamat, Mohd Basri Ali &amp; Omar Bapokutty</i>	103 - 113
Mechanical Properties of Cross-Ply Banana-Glass Fibre Reinforced Polypropylene Composites <i>Norizzati Zulkafli, Sivakumar Dhar Maligam, Siti Hajar Sheikh Md Fadzullah, Zaleha Mustafa, Kamarul Ariffin Zakaria &amp; Sivarao Subramonian</i>	114 - 125
Sound Insulation Performance of Kenaf Fibre as A Noise Control Treatment in Car Using Statistical Energy Analysis <i>Norzailan Azahari, Azma Putra, Reduan Mat Dan &amp; Muhammad Nur Othman</i>	126 - 139
Properties of Electrodeposited Nickel Cobalt Coated Mild Steel Developed from Alkaline Bath <i>Nik Hassanuddin Nik Yusoff, Othman Mamat &amp; Mahdi Che Isa</i>	140 - 150
Wear Behaviour of a-C:H Helical Gear Through Particle Generation <i>Abdul Hakim Abdul Hamid, Reduan Mat Dan, Azma Putra, Mohd Nizam Sudin &amp; Rozdman Khaidir Mazlan</i>	151 - 165



Ministry of Defence  
Malaysia

SCIENCE & TECHNOLOGY RESEARCH  
INSTITUTE FOR DEFENCE (STRIDE)

## **EDITORIAL BOARD**

### **Chief Editor**

Gs. Dr. Dinesh Sathyamoorthy

### **Deputy Chief Editor**

Dr. Mahdi bin Che Isa

### **Associate Editors**

Dr. Ridwan bin Yahaya

Dr. Norliza bt Hussein

Dr. Rafidah bt Abd Malik

Ir. Dr. Shamsul Akmar bin Ab Aziz

Nor Hafizah bt Mohamed

Masliza bt Mustafar

Kathryn Tham Bee Lin

Siti Rozanna bt Yusuf



# WEAR BEHAVIOUR OF a-C:H HELICAL GEAR THROUGH PARTICLE GENERATION

Abdul Hakim Abdul Hamid<sup>1,2</sup>, Reduan Mat Dan<sup>1,2\*</sup>, Azma Putra<sup>1,2</sup>, Mohd Nizam Sudin<sup>1,2</sup> & Rozdman Khaidir Mazlan

<sup>1</sup>Fakulti Kejuruteraan Malaysia

<sup>2</sup>Centre for Advanced Research on Energy  
Universiti Teknikal Malaysia Melaka (UTeM), Malaysia

\*Email: reduan.dan@utem.edu.my

## ABSTRACT

*This paper presents the wear performance of amorphous hydrogenated carbon (a-C:H) deposited on helical gears through wear debris analysis. Helical gears are tested on a power recirculating test rig with constant loads of 100 Nm and speed of 1,000 rpm. The tests are conducted for 9 million cycles or an initial pitting of 25% covering the surface of the teeth. Samplings are obtained for approximately 60 ml of the lubricant for every  $3.6 \times 10^5$  cycles, which are then analysed through oil analysis that includes wear debris analysis as well as particle counting. The results reveal that the a-C:H coated gear reduces the particle generation by a factor of 3.11 as compared to the baseline testing. However, a-C:H does not affect the condition of the lubricant. It is found that the a-C:H gear had reduction in micro-pitting formation as compared to the uncoated gear. This study demonstrates an extension of the life of gears through the application of a-C:H coating.*

**Keyword:** *Diamond-like carbon; helical gear; condition monitoring; fatigue life; power recirculating gear test rig.*

## 1. INTRODUCTION

Gears are one of the main mechanisms for power transmissions in almost all machines. The primary purpose of gear systems is to implement motion transmission, as well as to increase or to decrease the speed of shafts carrying rollers or loads. Recent developments on design and manufacturing of gearboxes strive for a more compact design that yields a larger capacity of power transmission. Due to the nature of the power transmission that involves variable speed of rotary mechanism and heavy loads, gears tend to experience failures at various cycle of the machine operation. The common failure modes of gear typically include bending fatigue, contact fatigue, scuffing, wear, cracking, fracture and plastic deformation (AGMA, 2014). However, countless analyses have identified that the factors in most occurring failure modes are tooth-bending fatigue, contact fatigue, scuffing and abrasive tooth wear (Edwards, 2004).

Surface technology is a feasible solution towards improving the service life of gears and is now extensively developed, which includes various methods such as surface hardening, shot penning and nitriding. Surface coating is a promising method to improve surface performance. The current generation of popular hard coatings is the “diamond like carbon” (DLC), where it has been proven to have profound tribological advantages in sliding-rolling contact components. Manier *et al.* (2010) found that the amorphous hydrogenated carbon (a-C:H) and the tetrahedral amorphous carbon (ta-C) coating surpasses the ceramic coating performance under slip rolling condition at a high Hertzian contact stress of 3.5 GPa. Various studies have also been conducted on the influence of DLC coatings towards the improvement of the common failure mode resistance, such as contact fatigue and scuffing resistance. Krantz *et al.* (2004) demonstrated an extension of life of tungsten DLC (a-C:H:W) coated

gears by a factor of six through accelerated fatigue testing. However, it is discovered that the performance of DLC coated gears changed with the load condition applied. Under low load conditions, the gears exhibited longer fatigue life, while in high load conditions, the fatigue life is comparatively shorter or equal to the non-coated gear (Fujii *et al.*, 2010). Although DLC coating provides an advantage on maximising resistance towards gear failures, the complex interactions for various parameters, such as the elastohydrodynamic lubrication (EHL), temperature and contact pressures yields various results of enhancements as well as deterioration.

The utilisation of a-C:H coating on the influence of gears is rarely discussed as most of the existing studies are conducted using a-C:H:W coating (Joachim *et al.*, 2002; Kalin & Vižintin, 2005; Kržan *et al.*, 2006; Michalczewski *et al.*, 2013a; Tuszynski *et al.*, 2015; Velmurugan & Vijayakumar, 2017). An experimental testing of a-C coating on cylindrical gears applied with a high contact stress was presented by Xiao *et al.* (2014), which suggested that the prolongation of the gear life is achievable by a factor of three. The study on a-C:H coating on spur gears lubricated under ecological oil is demonstrated by Michalczewski *et al.* (2013b), where the coated gears had an increased scuffing load capacity. Another a-C:H coating study was published by Fujii *et al.*, (2011), where fatigue testing is conducted on gears under vacuum condition. The study also suggested improved scuffing load capacity in comparison with the uncoated gear.

This paper focuses on the wear behaviour of a-C:H coated helical gear in terms of the wear debris generation as well as the surface fatigue formation. Its effect on the lubricant condition is also discussed.

## 2. METHODOLOGY

### 2.1 a-C:H Specification and Gear Specification

Prior to experimental investigation, the DLC coatings are selected based on the optimum condition for helical gear testing using pareto optimal analysis and weighted decision matrix. Tables 1 and 2 show the selected DLC coating and gear specification used in the experiment.

**Table 1: a-C:H specification.**

Coating	Material	Thickness range $\mu\text{m}$	Microhardness HV 0.05/ Hardness (GPa)	Coefficient of friction	Service temperature ( $^{\circ}\text{C}$ )	Deposition temperature ( $^{\circ}\text{C}$ )
Tribobond 43	a-C:H	1-5	2500-4000/ 12-20	0.1	300	160-200

The gears are made from low carbon steel (AISI 1020), which after hobbing are carburised at temperatures higher than 900  $^{\circ}\text{C}$  with an as-ground surface for the physical vapour deposition (PVD) deposition of the a-C:H coating. The standard specification of the AISI 1020 steel gives a hardness value of 130 HV, but through testing using a Shimadzu HVM-G Micro Vickers Hardness Tester, it was recorded that the core hardness was at 261 HV. Due to the low-cost consideration of gear fabrication, pack carburisation is utilised where the case depth proved to be difficult to control. Nevertheless, the range was approximately 1.2 to 1.5 mm. The carburised gear has a case hardness of 546 HV, whereby the a-C:H deposition has a case hardness of 769 HV. The adhesion layer of chromium (Cr) is deposited as an interlayer through the PVD process, which is followed by the deposition of a-C:H coating via plasma assisted chemical vapour deposition (PACVD) process. Table 1 and 2 shows the a-C:H specification as well as the test gear parameters respectively.

**Table 2: Gear specifications.**

	<b>Specifications</b>
<b>Type of Gear</b>	Helical
<b>Helix angle</b>	17.75
<b>Pressure angle</b>	20
<b>Centre to centre distance</b>	113 mm
<b>Module of gear</b>	3
<b>Number of teeth</b>	36
<b>Face width</b>	15 mm (preliminary) / 7 mm (pitting) / 3 mm (pitting)
<b>Tip diameter</b>	116.25 mm
<b>Pitch diameter</b>	110.25 mm
<b>Applied Tangential Loading</b>	1818 Nm
<b>Lubricant</b>	DEXRON III Pennzoil
<b>Gear Material</b>	AISI 1020, Casehardened

## 2.2 Selection of Machine and Experimental Setup

Figures 1 and 2 shows the setup and schematic diagram of the power recirculating test rig. The test rig for the wear analysis in the experiment utilised the power recirculating gear system consisting of four helical gears. The shafts have four stubs of 250 mm of length and 25 mm in diameter. As the gears were installed, the shafts were locked in a close loop mesh, which allowed torsional loading to be applied. A special coupling to apply torsion by twisting the stub on the driven shaft was introduced. The coupling consisted of two concentric flanges, in which one side of the coupling possessed a triangular platform where set screws forced the stubs to be twisted. This causes angular misalignment or commonly known as torsion, which in turn causes the gear to be loaded with tangential force. Accelerated wear is the aim for the construction of this type of test rig. The main shaft was fitted with a torque transducer via rigid couplings connected to the stubs, which measured the applied torsion for a precise loading. A 10 HP DC motor drove the main shaft with a variable speed of up to 2,900 rpm.



**Figure 1: Power recirculating test rig.**

Preliminary testing was conducted for a Hertzian contact stress of 551 and 957 MPa to identify the capacity of the test rig. The actual experiments were conducted under a loading of 1,231 MPa for 9 million cycles for both AISI 1018 carburised gear and a-C:H coated gear at a constant speed of 1,000 rpm and a lubricant starting temperature is at room temperature. Samples were taken for every  $3.6 \times 10^5$  cycles at approximately 60 ml per sample through the sampling port of the rig.

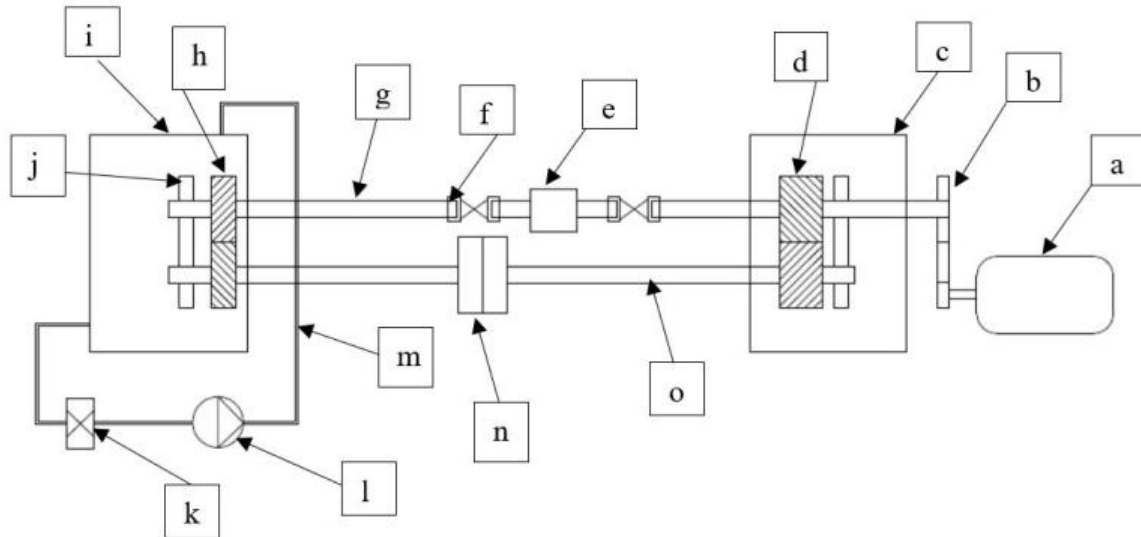


**Figure 2: Schematic diagram of the gear test rig with lubricant path. The elements are: [a] AC motor, [b] tooth belt, [c] slave gear oil sump, [d] slave gear, [e] torque transducer, [f] flexible coupling, [g] drive shaft, [h] test gear, [i] test gear oil sump, [j] needle bearing casing, [k] 10 µm oil filter, [l] magnetic pump, [m] lubricant path, [n] torsional coupling, [o] driven shaft.**

### 2.3 Wear Debris Analysis, Optical Imaging Analysis and Oil Analysis

The collected samples were analysed using a CSI Spectro 5200 trivector analyser for wear debris analysis and Q1000 Fluidscan for oil analysis using IR spectroscopy. Both equipment adhere to ASTM D7416 and ASTM D7889 respectively. A Dino-Lite AM4515 digital microscope was used to capture the surface conditions of both the uncoated and coated gears for the natural progression of pitting under accelerated loading conditions at the same interval as lubricant sampling. The results were then compared for both the uncoated and coated gears with progression of up to 9 million test cycles. At the end of the test cycles, as Axioskop 2 optical image analyser was utilised to capture the surface of isolated tooth at a 5x to 100x magnification for both gear surface conditions. The determination of the cumulative wear rate is given by:

$$Wear\ rate = \frac{Q \times M}{t_t - t_{t-1}} \quad (1)$$

where  $Q$  is the number of cumulative particles counted,  $M$  is the cumulative mass of the particles and  $t_t - t_{t-1}$  is the cycle of gear revolution for each test. The cumulative wear is used to determine the wear stages of both gear surface conditions through the quantitative analysis of particle counting.

## 3. RESULTS AND DISCUSSION

The overall wear performance in each test is assessed from the progression of micro-pitting damage, particle generation and lubricant condition. The results are limited to the formation of micro-pitting on the surface of the gear for both the uncoated and coated gear due to the test rig having a limitation of a low load output.

### 3.1 Particle Generation of Micro-Pitting Damage

The most significant factor in the particle generation is the ferrous index, which determines the ferrous composition of the particles dispersed in the lubricant. It is noted that the progressive nature of the micro-pitting on gear surfaces is a crucial feature for determining the wear performance of a gear under contact fatigue damage, thus provides useful information for predictive maintenance (Moorthy & Shaw, 2012).

Figures 3 to 5 present the particle generation for both the uncoated and coated gear. The particles are divided into three size categories, namely small diameter (SD), medium diameter (MD) and large diameter (LD). The details are listed in Table 3. The SD particles are associated but are not limited to various wear mechanisms comprising of rubbing wear, cutting wear, combined rolling and sliding wear as well as rolling fatigue, which involve pitting and spherical particles. However, SD particles are more prominent in the generation of spherical particles, which is generated through rolling fatigue wear and rubbing wear. These wear modes generally produce particles with sizes of 3 to 10  $\mu\text{m}$  and 5 to 15  $\mu\text{m}$  respectively.

**Table 3: Particle size categories.**

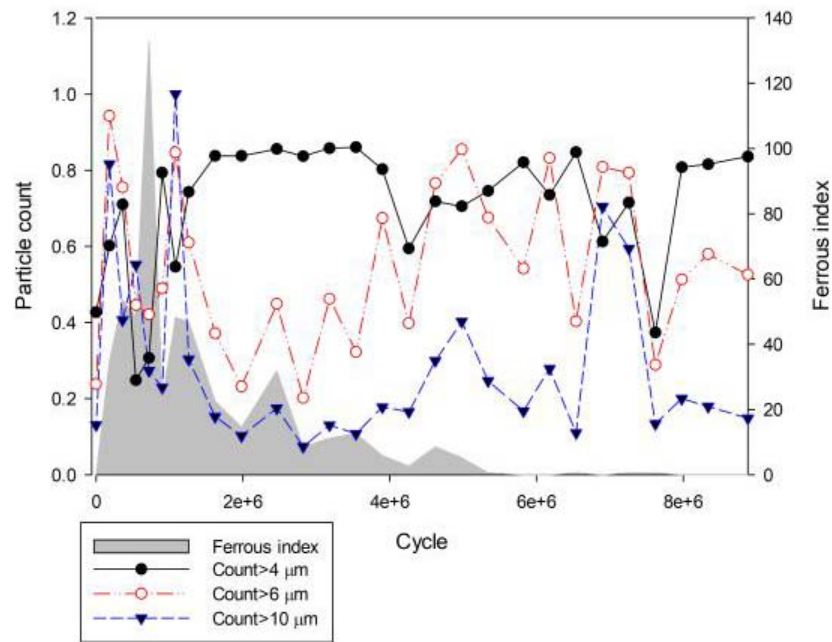
Particle Diameter	Size
Small Diameter (SD)	$\leq 10 \mu\text{m}$
Medium Diameter (MD)	$\leq 28 \mu\text{m}$
Large Diameter (LD)	$\geq 32 \mu\text{m}$

The MD particle generation categorised by its sizes are the result of various wear mechanisms faced by the gear during its operational life. The wear mechanism includes cutting wear, rolling fatigue generating spall and laminar particles, as well as combined rolling and sliding wear. However, MD particles is determined to be generated prominently via rolling fatigue generating laminar particles, and combined rolling and sliding wear, where both mechanisms produce particles of sizes 20 to 50  $\mu\text{m}$  and 2 to 20  $\mu\text{m}$  respectively. The combined rolling and sliding wear generate a complex fusion of particle morphology and thus, it is difficult to be categorised by size only. It is also worthy to note that severe sliding wear occurs only in MD particle sizes onwards. The wear modes resulting in the generation of the LD particles are determined to be of rubbing wear, cutting wear, rolling fatigue producing spall and laminar particles, and severe sliding wear (Anderson *et al.*, 1991).

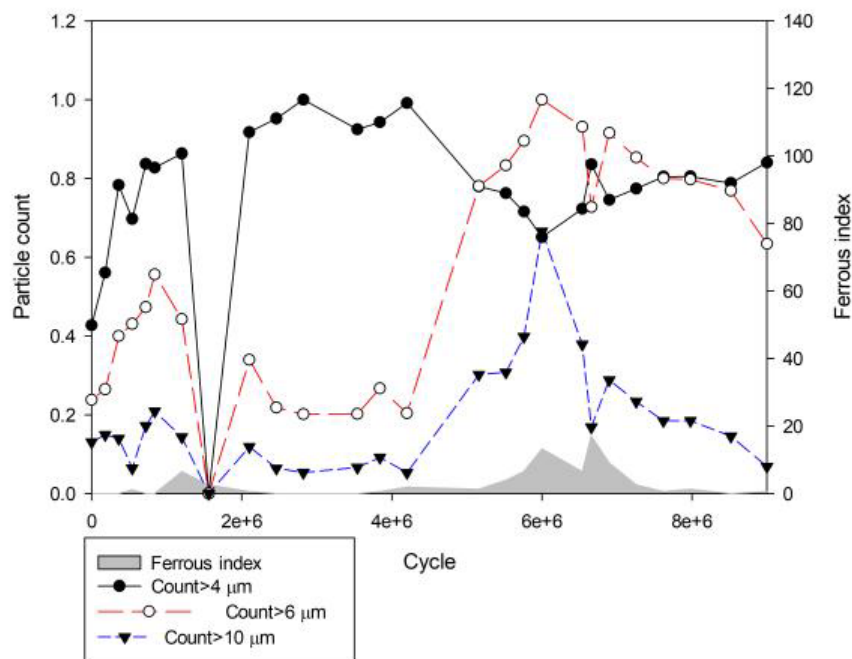
Ferrous index is sensitive to conductive, ferromagnetic particles that increase linearly with both particle size and concentration. The index measures recent, severe wear of oil-wetted steel and iron parts due to the surfaces of such particles that are likely to be conductive. Figure 3 shows the SD particle distribution. For the uncoated gear, the ferrous index was observed to increase significantly at the start of the test reaching a maximum ferrous index value and then decreased rapidly until the test reached 5.34 million test cycles. A small value of ferrous index is then observed at 6.54 million test cycles and between 7.26 and 7.62 million test cycles. The ferrous index measurements suggest that the particles generated at this specific point in the gear life cycle are of ferrous composition. As for the coated gear, the ferrous index remains at lower values observed throughout the gear cycles, which indicates that very little concentration of ferrous particles was removed from the coated gear gradually over the test cycle. Most of the particles are of non-ferrous composition.

The results in Figure 3 determines that the uncoated gear experienced wear mechanisms that are assumed to be rolling fatigue wear and rubbing wear. Uncoated gears produced larger particle sizes of 6 and 10  $\mu\text{m}$  in the SD particle distribution as compared to those from the coated gear. Possible particle morphologies generated for these particle sizes include spherical particles and platelets (Anderson *et al.*, 1991). Similar trends can also be observed for the case of MD and LD particles in

Figures 4 and 5 respectively. For the MD particles, the possible particle morphologies would be of laminar particles, striated particles, and a complex fusion of wear debris due to combined rolling and sliding wear. For the LD particles, the possible particle morphologies experienced are spherical, ribbons, chunks, platelets and striated particles, as shown in Figure 6.



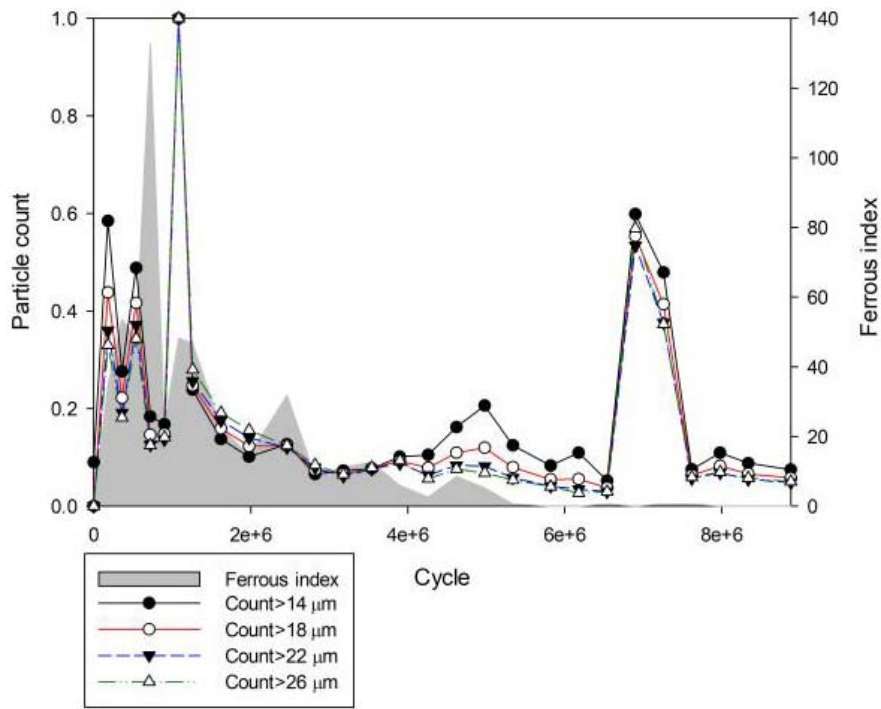
(a)



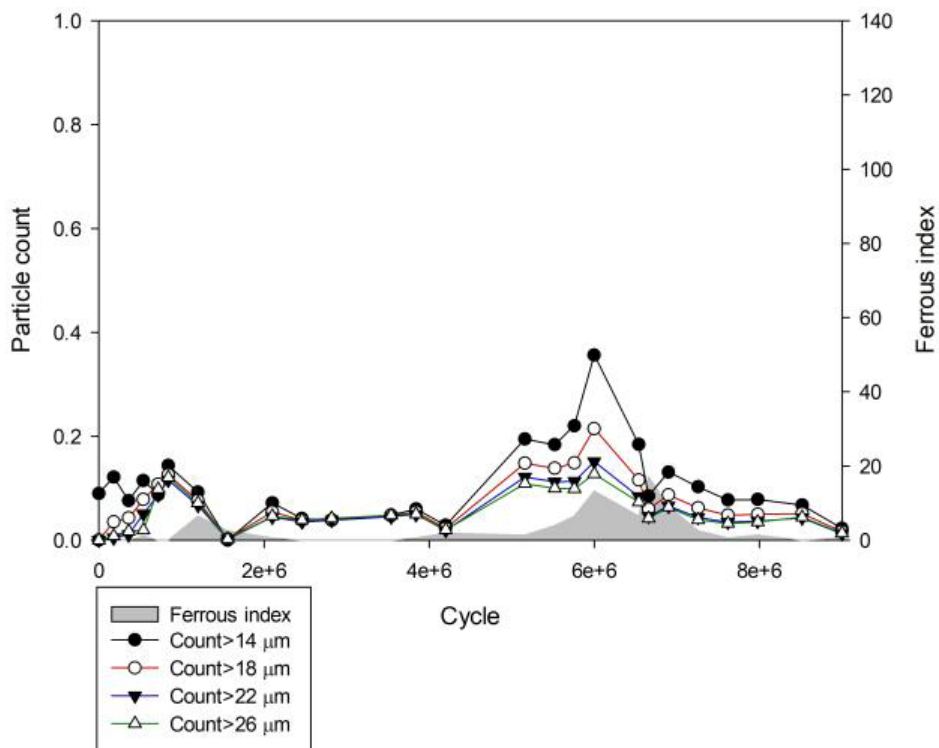
(b)

Figure 3: Small diameter (SD) particle generation progression: (a) AISI 1020 carburised and (b) a-C:H coated AISI 1020 carburised.



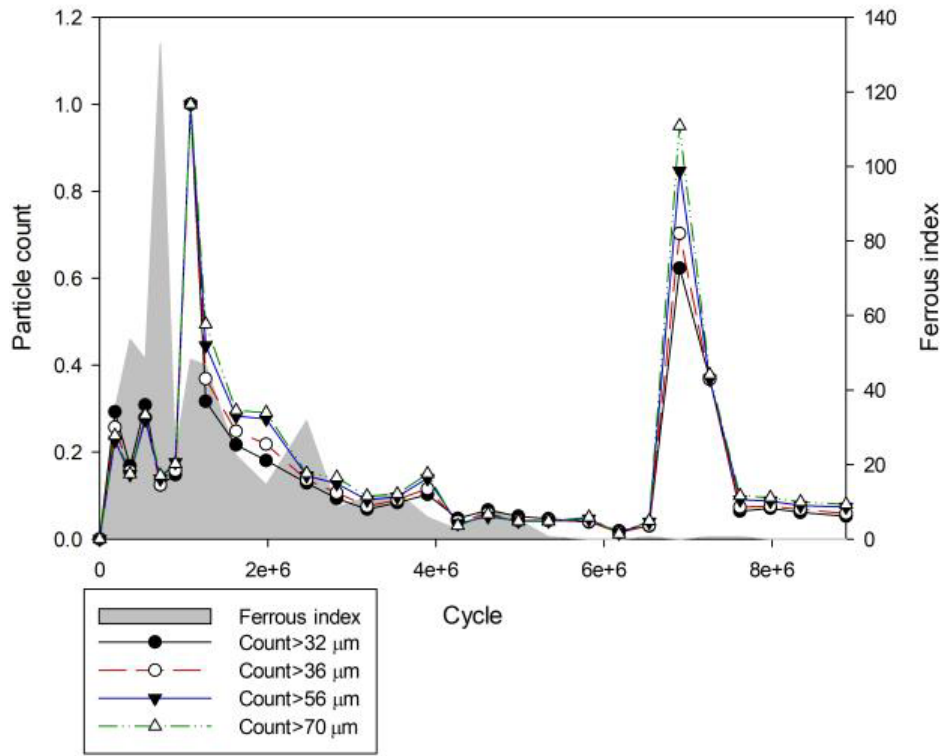


(a)

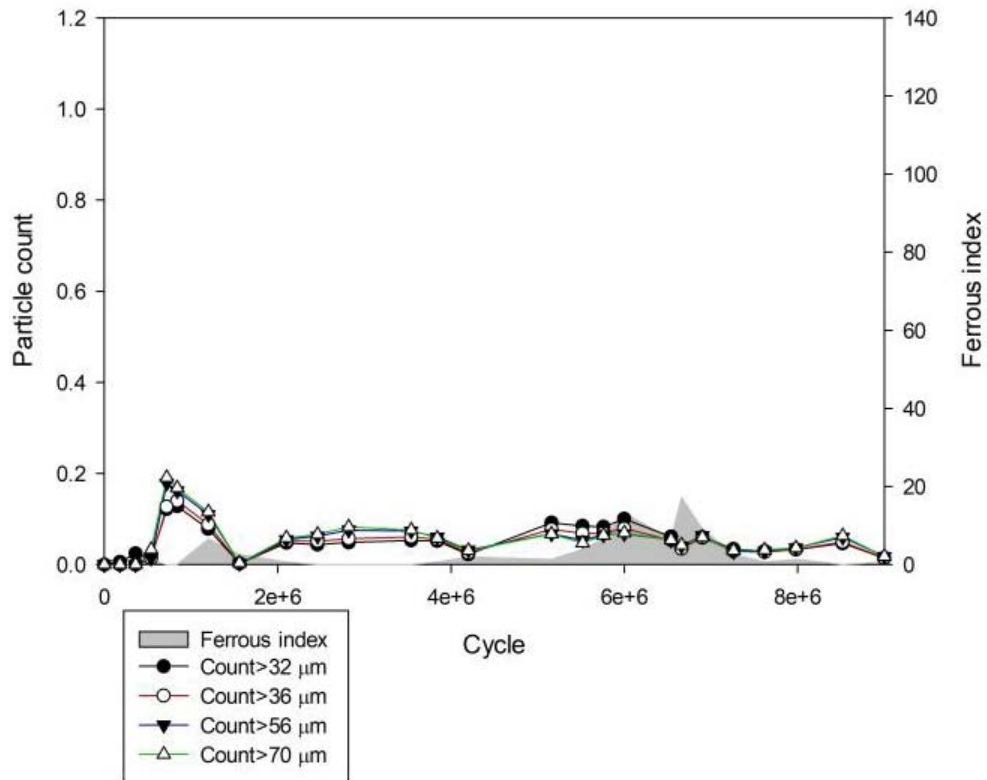


(b)

**Figure 4: Medium diameter (MD) particle generation progression: (a) AISI 1020 carburised and (b) a-C:H coated AISI 1020 carburised.**



(a)



(b)

Figure 5: Large diameter (LD) particle generation progression: (a) AISI 1020 carburised and (b) a-C:H coated AISI 1020 carburised.

A cumulative wear rate of all the particle sizes are compared for the coated and uncoated gears as shown in Figure 7. From the trend, it can be clearly observed that the uncoated gear had three wear stages, which are run-in wear, steady-state wear and the initial failure zone, while the coated gear has an extended run-in wear that leads to a steady state wear. The run-in zone for the uncoated gear was determined to last for  $1.62 \times 10^6$  gear revolutions, which then entered a steady state wear that lasted for  $5.04 \times 10^6$  revolutions and subsequently entered an initial failure at  $6.54 \times 10^6$  of gear revolution.

The coated gear showed an absolute divergence of wear debris generation behaviour as the run-in zone extended for  $6.66 \times 10^6$  revolutions and then entered the steady state wear. This behaviour is consistent with the gear surface damage shown in Figures 9 and 10, which is discussed in more detail in Section 3.3. This finding determines the prolongation of the helical gear life by a factor of 3.11 through running-in quantification comparison.

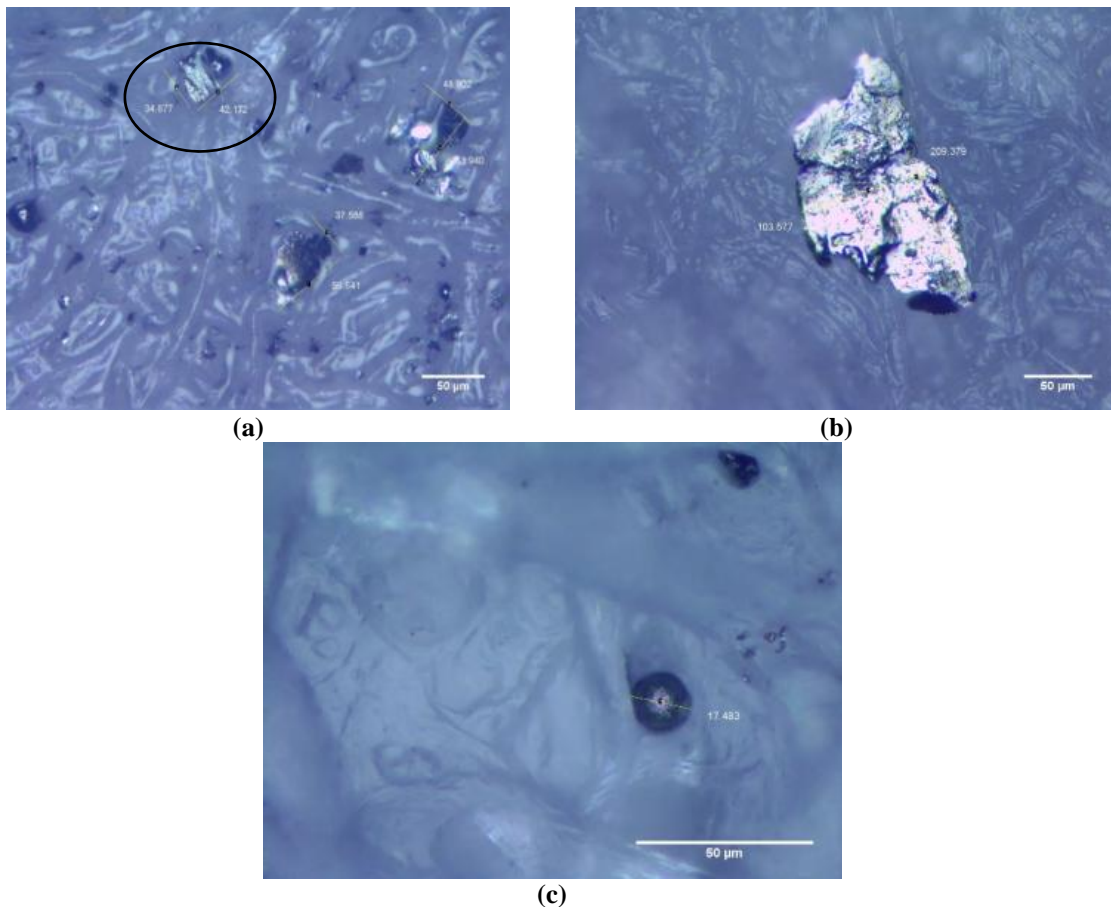


**Figure 6: Wear debris particles: (a) Platelets (annotation indicates platelets with striation marks)  
(b) Chunks (c) Spherical.**

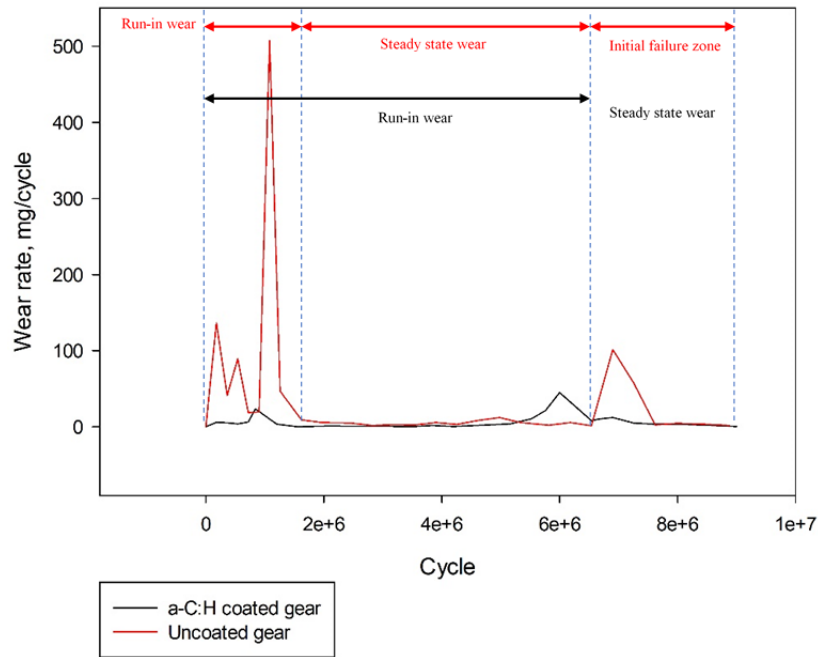


Figure 7: Cumulative wear rate of a-C:H coated gear vs uncoated gear.

### 3.2 Oil Analysis

The a-C:H coating has an insignificant impact on the condition of the lubricant, where the oxidation and viscosity has miniscule enhancement as compared to the uncoated gear lubricant through the progression of the test cycles, which can be observed in Figure 8. The uncoated gear has oxidation level ranges from 19.2 to 20.1 abs/0.1 m, while for the coated gear, it ranges from 19.3 to 19.9 abs/0.1 m. The degradation of oil due to oxidation or ageing is mainly caused by high temperatures of the lubricant, thus the behaviour shown in these experiments suggests that a high temperature during the experimentation did not occur.

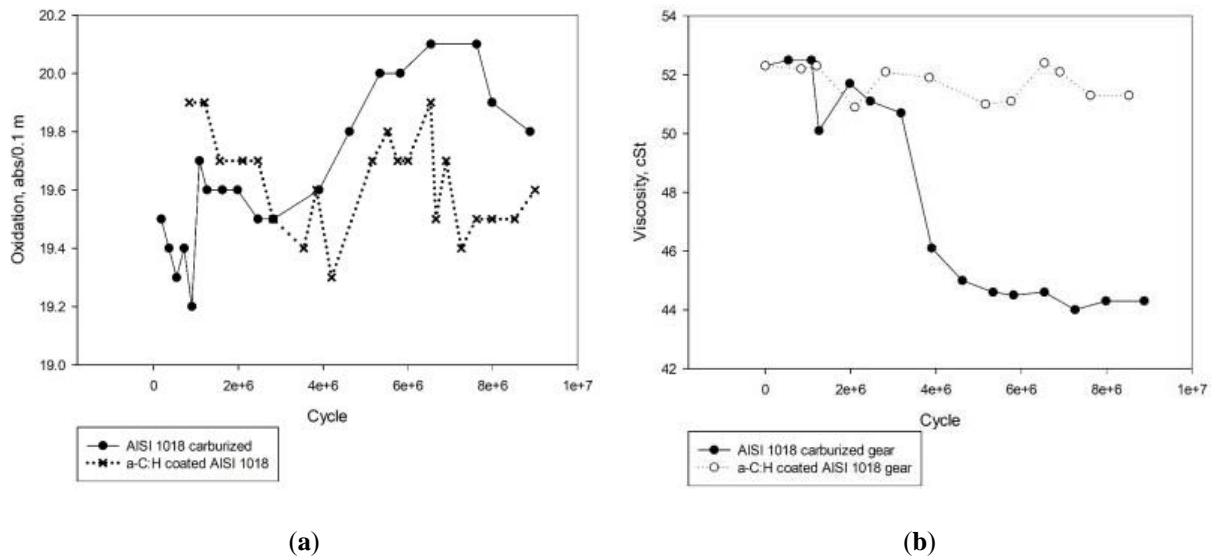
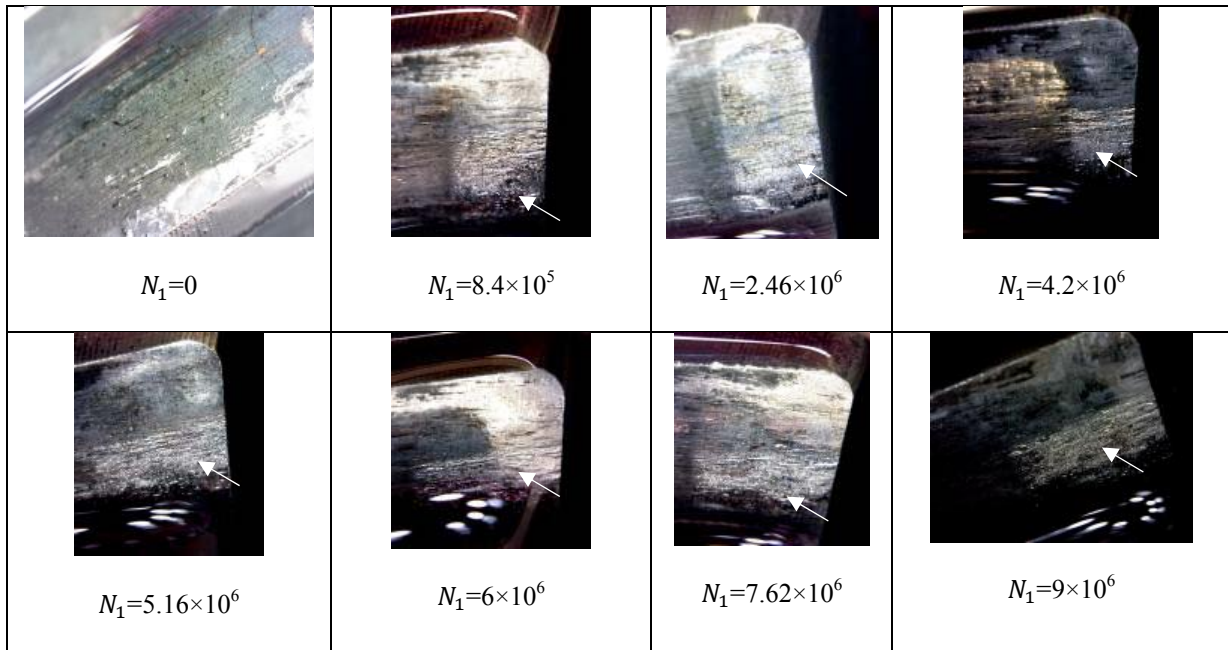


Figure 8: Oil analysis of a-C:H coated gear vs uncoated gear: (a) Oxidation (b) Viscosity.

However, the viscosity of the lubricant differs from the influence of oxidation, where the uncoated gear debilitates over the course of the test cycle, while the viscosity of the coated gear remains constant towards the end of the experiment. As high temperature did not occur during the experiment, this result suggests that the uncoated gear lubricant may contain contamination.

### 3.3 Gear Tooth Image Analysis

Figures 9 and 10 present the gear surface image captured for the  $N^{\text{th}}$  test cycle. From the images, the wear mode can be identified with the formation of micro-pitting.



**Figure 9: AISI 1020 carburised uncoated gear surface image (the arrows annotate the formation of micropitting).**

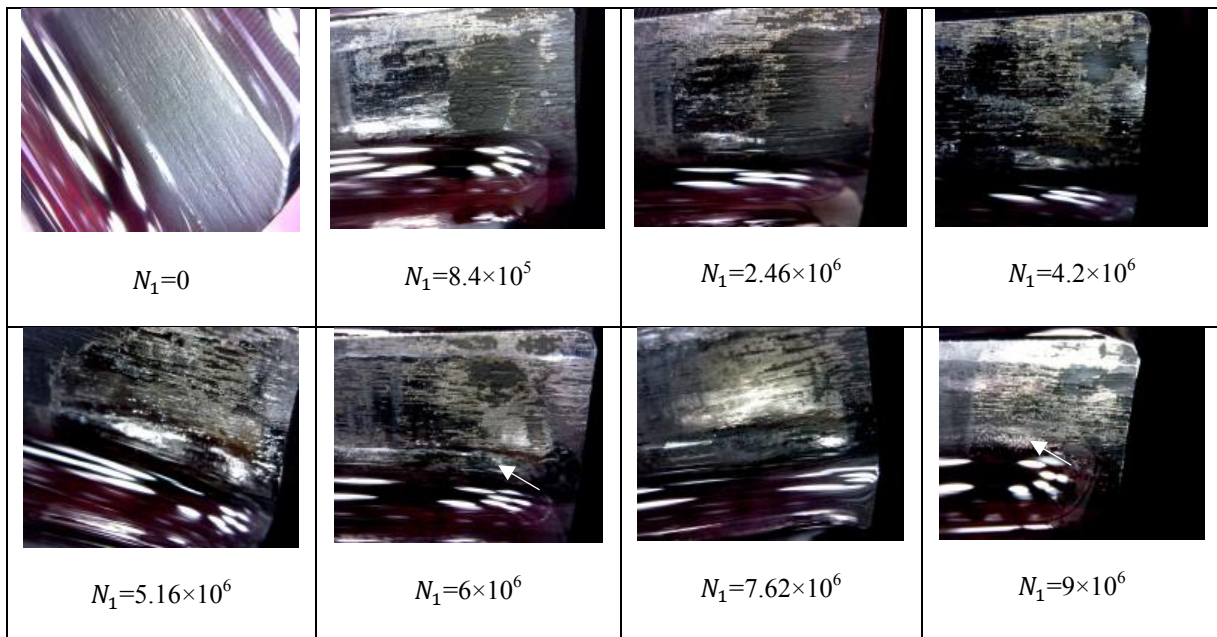


**Figure 10: a-C:H coated AISI 1018 carburised gear surface image (the arrows annotate formation of micropitting).**



A significant difference can be observed as the formation of micro-pitting occurred at an earlier cycle for the uncoated gear in Figure 9, while in Figure 10 the coated gear is shown to have experienced peeling at the earlier cycle and micro-pitting occurred only at  $6 \times 10^6$  cycles onwards.

Through this observation, it is revealed that the a-C:H coating improves the scuffing and pitting resistance of the coated gear substantially in comparison with the uncoated gear where for the latter, prominent formation of micropits and scuff marks are scattered throughout the gear teeth. For the peak contact stress of 1,231 MPa in the experiment, it is found that for the uncoated gear, the generation of surface damage occurred frequently on the dedendum, indicating that the most severe mesh sliding condition prevail similar to the study demonstrated by Fernandes & McDuling (1997).

The uncoated gear showed progressive micropitting observed at the dedendum of the gear, which includes the gear tooth root and contact pitch line, as shown from optical imaging of the gear surface in Figures 11 (b) and (c). It can also be observed that scuffing mark occurrence is more prominent in the contact pitch line, lessens at the tooth root and is non-existent at the tooth tip. Microcracks are also observed solely at the tooth tip, which is also a sign of the initiation of micropits, as shown in Figure 11 (a).

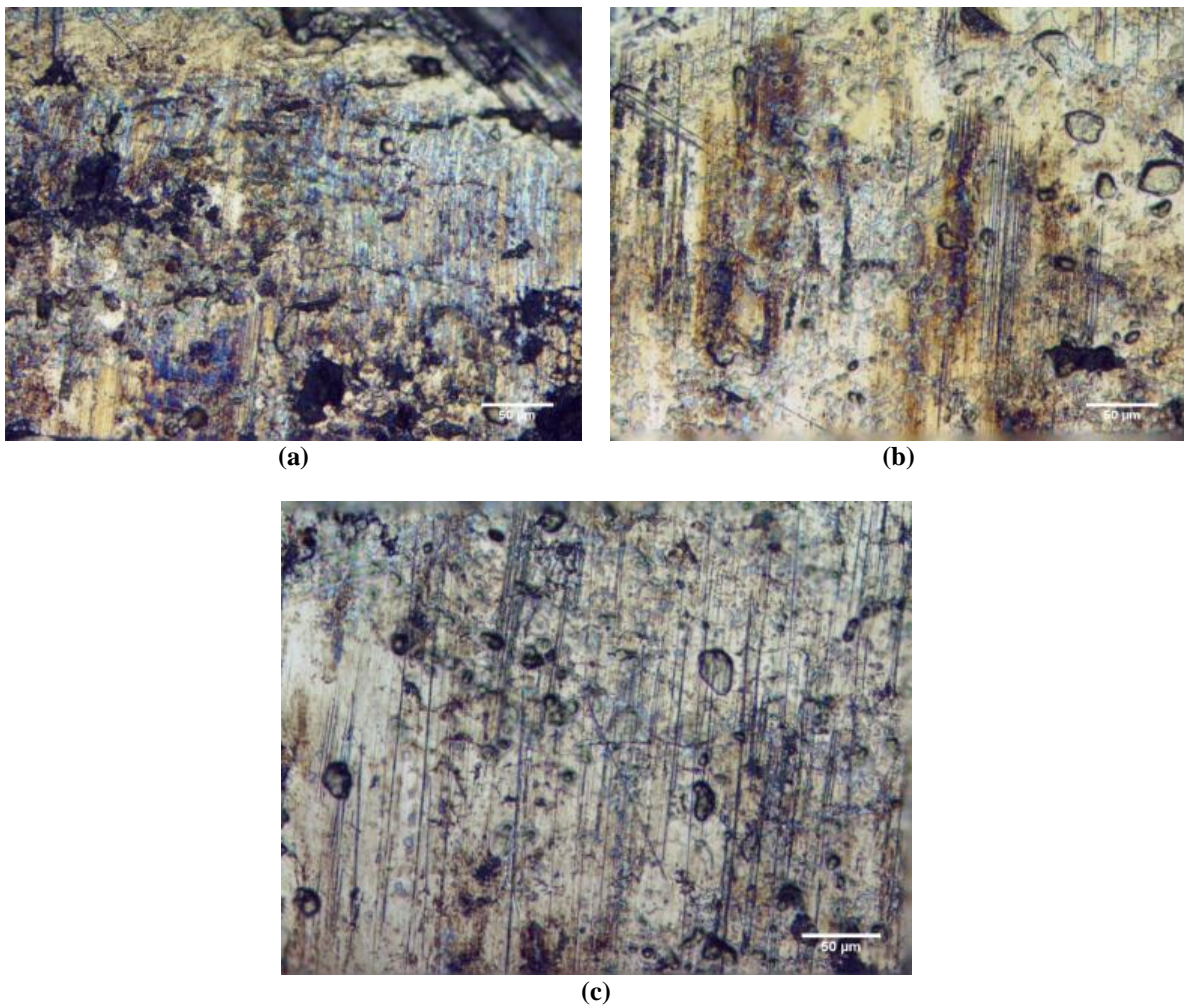


**Figure 11: Optical stereo images of uncoated gear surface at the end of the test with peak contact stress of 1,231 MPa: (a) Tooth tip (b) Tooth root (c) Contact pitch line.**

The a-C:H coated gear exhibited completely different damage on its surface, where micropitting and scuffings are observed solely on the gear tooth tip, as shown in Figure 12 (a) albeit at a smaller scale and the coating partially remained intact. The tooth root suffered from large scale microcracks at the end of the test with partial peeling of the coating observed, as shown in Figure 12 (b). At the contact pitch line of the gear, no microcracks are observed.

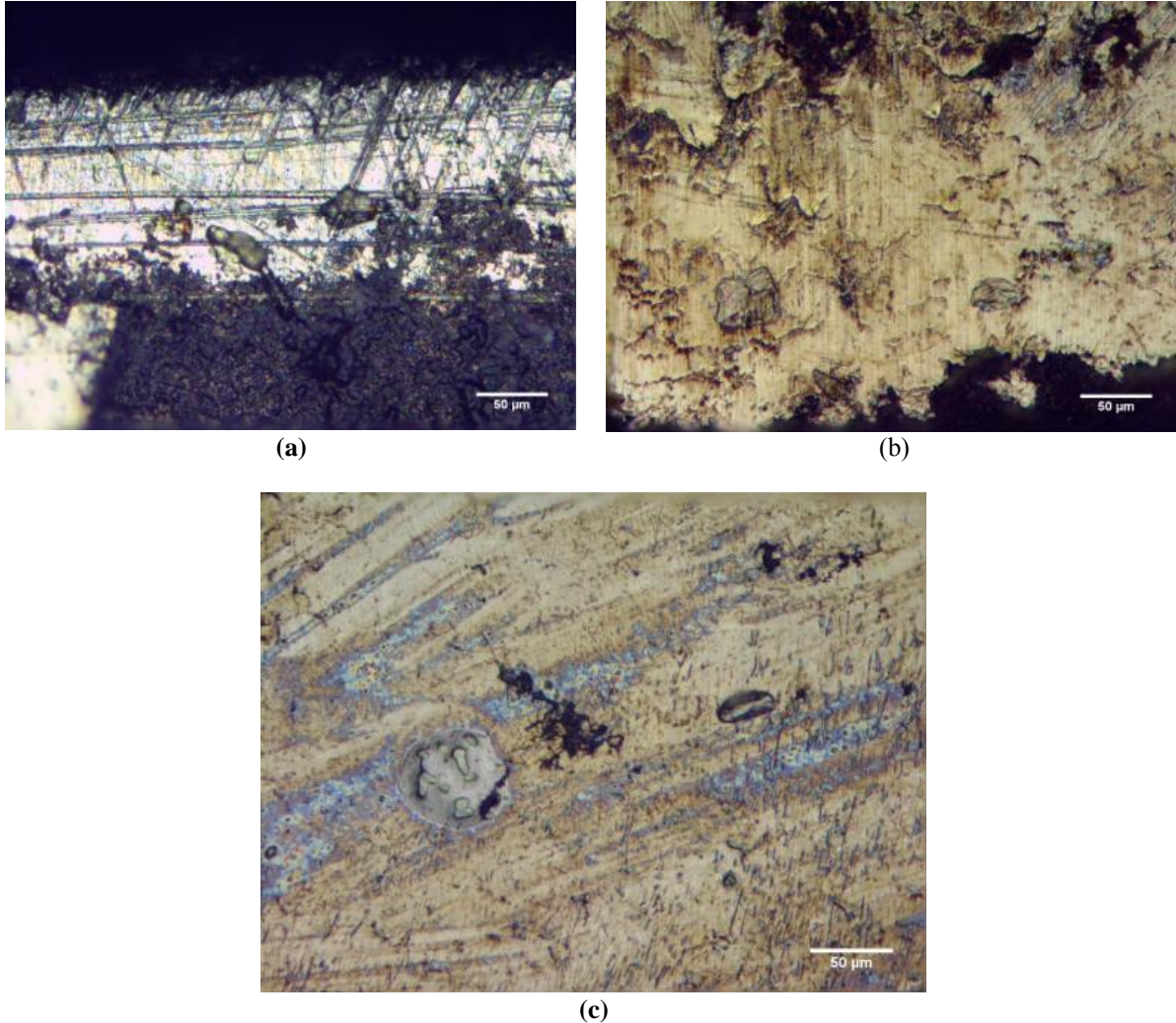


**Figure 12: Optical stereo images of coated gear surface at the end of the test with peak contact stress of 1,231 MPa: (a) Tooth tip (b) Tooth root (c) Contact pitch line.**

The surface of the gear became smoother as a result of the interaction of the coating and gear surface after extended sliding and rolling mechanisms (Moorthy & Shaw, 2013). The surface coating is found to be completely removed as shown in Figure 12 (c). However, a polished surface would promote a decrease in material removal of the surface gear as no asperities or valleys are involved during the sliding and rolling mechanism of the gear.

#### **4. CONCLUSION**

The wear behaviour of a-C:H coated AISI 1018 carburised gear at peak Hertzian contact stress levels of 1,231 MPa in Pennzoil oil using power recirculating gear test rig was discussed in this manuscript. The results strongly suggest a significant improvement towards wear resistance of the carburised AISI 1018 gear. Through the particle generation analysis, it was concluded that the a-C:H coating influences the wear stages of the gear, where it was found that the running-in wear was experienced at

a relatively low wear rate with an extended cycle in comparison with the baseline testing. It was revealed that the a-C:H coating improved the life of the gear by a factor of 3.11 as compared to the uncoated gear. The a-C:H coating was observed to have no influence on the degradation of the gear lubricant. Peeling also occurred due to low adhesion between the deposited a-C:H and gear surface. The reduction of micro-pitting was significant for the a-C:H coated gear, which in our study occurred at  $6 \times 10^6$  cycles. Thus, it can be concluded that a-C:H coating improved the material removal rate of the gear leading to a low wear debris generation due to its properties of high hardness and low coefficient of friction.

## ACKNOWLEDGEMENT

This work was supported by the grant from the Ministry of Education of Malaysia (Grant RAGS/1/2014/TK01/FKM/B00070). The authors acknowledge the contributions from Universiti Teknikal Malaysia Melaka (UTeM) and the members of the Vibration and Structural Health Monitoring (ViBRO) research group.

## REFERENCES

- AGMA (American Gear Manufacturer Association) (2010). *ANSI/AGMA 1010-F14 Appearance of Gear Teeth-Terminology of Wear and Failure*. American Gear Manufacturer Association, Washington, D.C.
- Anderson, D.P., Bowen, E.R. & Wescott, V. C. (1991). *Wear Particle Atlas*. Spectro Incorporated Industrial Tribology Systems, Chelmsford, Massachusetts.
- Fernandes, P.J.L. & McDuling, C. (1997). Surface contact fatigue failures in gears. *Eng. Fail. Anal.*, **4**: 99–107.
- Fujii, M., Ananth Kumar, M. & Yoshida, A. (2011). Influence of DLC coating thickness on tribological characteristics under sliding rolling contact condition. *Tribol. Int.*, **44**: 1289–1295.
- Fujii, M., Seki, M. & Yoshida, A. (2010). Surface durability of WC/C-coated case-hardened steel gear. *J. Mech. Sci. Technol.*, **24**: 103–106.
- Joachim, F., Kurz, N., & Glatthaar, B. (2002). Influence of coatings and surface improvements on the lifetime of gears. *VDI BERICHT*, **2**: 565–582.
- Kalin, M., & Vižintin, J. (2005). The wear and temperature behaviour of DLC-coated gears lubricated with biodegradable oil. *VDI BERICHT*, **259**: 1005–1019.
- Krantz, T., Cooper, C., Townsend, D., & Hansen, B. (2004). Increased Surface Fatigue Lives of Spur Gears by Application of a Coating. *J. Mech. Design*, **126**: 1047.
- Kržan, B., Kalin, M. & Vižintin, J. (2006). The Lubrication of DLC Coated Gears with Environmentally Adapted Ester-Based Oil. *Int. Conf. Gears*, Düsseldorf, Germany, pp. 1345-1353.
- Manier, C.A., Theiler, G., Spaltmann, D., Woydt, M. & Ziegele, H. (2010). Benchmark of thin film coatings for lubricated slip-rolling contacts. *Wear*, **268**: 1442–1454.
- Michalczewski, R., Kalbarczyk, M., Michalak, M., Piekoszewski, W., Szczerek, M., Tuszynski, W., & Wulczynski, J. (2013a). New scuffing test methods for the determination of the scuffing resistance of coated gears. *Tribology-Fundamentals and Advancements, Intech, Croatia*, 187–215.
- Michalczewski, R., Szczerek, M., Tuszy, W., & Antonov, M. (2013b). The effect of low-friction PVD coatings on scuffing and pitting resistance of spur gears. *Tribologia*, **5**: 8–11.
- Moorthy, V., & Shaw, B. A. (2012). Contact fatigue performance of helical gears with surface coatings. *Wear*, **276**: 130–140.
- Moorthy, V. & Shaw, B.A. (2013). An observation on the initiation of micro-pitting damage in as-ground and coated gears during contact fatigue. *Wear*, **297**: 878–884.
- Tuszynski, W., Kalbarczyk, M., Michalak, M., Michalczewski, R., & Wieczorek, A. (2015). The effect of WC/C coating on the wear of bevel gears used in coal mines. *Mater Sci-Medzg*, **21**:



358–363.

Velmurugan, B., & Vijayakumar, S. (2017). Experimental Analysis of Hard Coating on Spur. *International Journal of Advances in Production and Mechanical Engineering*, **3**: 3–8.

Xiao, Y., Shi, W. & Li, L. (2014). Fatigue performance of cylindrical gearing with DLC coatings. *Int. Gear Conf. 2014*, Lyon, France, pp. 516–522.

Edwards, K. (2004). ASM handbook, volume 11: Failure analysis and prevention. *Mater. Design*, **25**: 735-736.